Electric Vehicle Participated Electricity Market Model Considering Flexible Ramping Product Provisions

Xian Zhang, Jiefeng Hu, Huaizhi Wang, Guibin Wang, Ka Wing Chan, Jing Qiu

***Abstract*—This paper studies Electric Vehicle (EV) potential to participate in the energy market and provide flexible ramping products (FRPs). EV traffic flows are predicted by the deep belief network, and the availability of flexible EVs is estimated based on the predicted EV traffic flows. Then, a novel market mechanism in distribution system is proposed to encourage the dispatchable EV demand to react to economic signals and provide ramping services. The designed market model is based on locational marginal pricing (LMP) of energy, and marginal pricing of FRPs. System ramping capacity constraints and EV operation constraints are incorporated in the proposed model to achieve the balance between the system social cost minimization and the EV traveling convenience. Moreover, typical uncertainties are considered by the scenario-based approach. Finally, simulations are conducted to verify the effectiveness of the established model and demonstrate the contributions of EVs to the system reliability and flexibility.**

***Index Terms*—Electric vehicle, demand management, flexible ramping product, locational marginal price, deregulated electricity market.**

NOMENCLATURE

A. Sets

Ω^{T} Set of all time subperiods.
Ω^{EA} Set of electric vehicle (EV) aggregators.
Ω^{B} Set of all system nodes.
Ω^{noEA} Set of system nodes except the nodes of Ω^{EA}.
Ω^{D} Set of nodes with dispatchable demands in Ω^{noEA}.
Ω^{S} Set of substations.
Ω^{k} Set of EV aggregators in zone k.

B. Parameters

D_t Duration of subperiod t.
c_i^{raup} The marginal cost of ramp power for EV aggregator i.
$U_m^{\max}$, $U_m^{\min}$ Maximum and minimum acceptable voltage magnitude of node m.
G_{mn}, B_{mn} Conductance and susceptance of feeder mn.
$P_{i,t}^{\mathrm{U}}$ Fixed power the EV aggregator i offers to EVs at time t.
$P_{m,t}^{\mathrm{F,max}}$, $P_{m,t}^{\mathrm{F,min}}$ Maximum and minimum demand of $P_{m,t}^{\mathrm{F}}$.
$P_{i,t}^{\mathrm{FL,max}}$, $P_{i,t}^{\mathrm{FL,min}}$ Maximum and minimum demand of $P_{i,t}^{\mathrm{FL}}$.
$R_{i,t}^{\mathrm{raup,max}}$ Upward ramp rate of EV aggregator i at time t.
Δ_i The physical ramp rate of EV aggregator i.
R_t^k Ramping rate requirements in zone k at time t.
P_i^{max} Maximum power of EV aggregator i.
S_m Apparent power capacity of the existing substation at node m.
S_{mn}^{Max} Designed transfer capacity of feeder mn.
η_i^{chg} The discharge efficiency of EV aggregator i.
$Soc_i^{\min}$ Minimum energy SOC of EV aggregator i.
$Soc_i^{\max}$ Maximum energy SOC of EV aggregator i.
Soc_i^{req} Required energy SOC of EV aggregator i.
T The time duration of a time period.
K The number of FRP zones.

C. Variables

$Soc_{i,t}$ Energy SOC of EV aggregator i
$e_{i,t}^{raup}$ the ramp capacity of EV aggregator i for upward FRP in period t.
$p_{i,t}^{\mathrm{L}}$ Distribution locational marginal price (LMP) of the node where EA i locates at time t.
$p_{m,t}^{\mathrm{L}}$ Distribution LMP of node m at time t.
p_t^{S} Electricity price of the balance bus at time t.
$P_{i,t}$ Active power EV aggregator i offered to EVs at time t.
$P_{m,t}^{\mathrm{S}}$, $Q_{m,t}^{\mathrm{S}}$ Active and reactive power provided by the substation at node m at time t.
$P_{m,t}^{\mathrm{L}}$, $Q_{m,t}^{\mathrm{L}}$ Active and reactive power demand at node m at time t.
$P_{m,t}^{\mathrm{noEA}}$ Active power demand at node m of Ω^{noEA} at time t.
$P_{m,t}^{\mathrm{D}}$ Dispatched active power demand at node m of Ω^{D} at time t.
$P_{i,t}^{\mathrm{FL}}$ Dispatched power EV aggregator i offered to EVs at time t.
$R_{i,t}^{\mathrm{raup}}$ The ramp power provided by the EV aggregator i at time t.
$U_{m,t}$, $U_{n,t}$ Voltage magnitude at node m and n at time t.
$P_{mn,t}$, $Q_{mn,t}$ Active transmission power and reactive transmission power of feeder mn at time t.
$\theta_{mn,t}$ Deviation of phase angle between node m and n at time t.

I. INTRODUCTION

Electric vehicles (EVs) will be important components in the future smart power and the transportation system to increase the efficiency of energy utilization and realize energy

X. Zhang is with the School of Mechanical Engineering and Automation, Harbin Institute of Technology, Shenzhen, 518055, China.
J. Hu (*Corresponding author*) is with the School of Science, Engineering and Information Technology, Federation University Australia, Mount Helen, 3353 VIC, Australia (e-mail: j.hu@federation.edu.au).
H. Wang, G. Wang are with College of Mechatronics and Control Engineering, Shenzhen University, Shenzhen, 518060, China.
K. W. Chan is with Department of Electrical Engineering, The Hong Kong Polytechnic University, 999077, Hong Kong, China.
J. Qiu is with the School of Electrical and Information Engineering, The University of Sydney, Camperdown, NSW, 2006, Australia.

sustainable development [1]. Meanwhile, batteries of EVs become promising energy storage due to their special characteristics of quick response, good extensibility and easy maintenance [2][3], which has drawn interests of many researchers. In the content of electricity markets, batteries of EVs could gain profits by providing various services in energy market [4], regulation market [5], or reserve market [6]. A decision support algorithm and energy market participation policy are developed for EV aggregators using dynamic programming in [4]. A joint power management of EVs and a data center for frequency regulation is considered in [5], and a market planning strategy is proposed to minimize energy cost and maximize regulation service revenue. In [6], a bidding strategy for the EV aggregator is proposed to maximize its profits from participating in different regulating reserves markets, and the results indicate the system operator attains cost savings while the aggregator divides its resources between the reserve market and the energy market.

The net load ramps, which are mainly caused by high penetrations of renewables, bring new challenges to power system operations to meet energy imbalances that could arise in the future [7]. In recent years, the concept of a new market product, the flexible ramp product (FRP), has been developed to deal with the increasing variability of net load ramps [8]. FRPs are firstly implemented by California independent system operator (ISO) and Midcontinent ISO in the USA, and the feature of FRPs is to enhance dispatch flexibility to maintain the energy balance threatened by the arising uncertainties of net load [9-11]. The FRPs are incorporated into the real time energy dispatch market in [12], and a risk-limiting economic dispatch model is used to optimize the dispatch and the provisions of FRPs. It is revealed in [13] that the PFRs in real-time ISO market could increase market efficiency and reduce the system operation cost. However, all the researches mentioned focus on transmission system and do not study the market mechanism with FRPs in the distribution system.

By far, conventional generators are the most common resource for providing FRPs, which are proved effective in reducing load and supply curtailments and improving the efficiency of electricity markets [14]. However, the deployment of fast-start generators in real-time to provide enough ramp capacity is usually expensive [15]. Wind generator is an alternative way to give ramp services economically, and it is found in [16] the wind power can benefit by providing ramp capacity due to their low marginal cost, which will also help wind power avoid curtailment. It is found in [17] that the wind power ramping product could also enhance the power system reliability, and wind power forecasts are important in providing high-quality ramping service. In [18], battery energy storage system (BESS) is utilized to optimally provide FRP in day-ahead energy and reserve markets, which demonstrates good profitability by allocating resources among various ancillary products. Compared with BESS, batteries of EVs have similar characteristics of good controllability and quick responsibility.

Due to the mobility nature of EVs, the available EVs should be estimated at first. It is a common practice to obtain the EV numbers in the EV aggregators indirectly from the traffic flow (TF) information [19-22]. Therefore, the accurate forecast of traffic flow at the candidate EV aggregator locations is the first and important step for the operation of EV aggregator and distribution system. Generally, this forecast could be influenced by different factors such as charging infrastructure, socioeconomic level and the government policy, many of which are not easy to be quantified. Multilayer neural network (NN) solves problems in a way similar to the human brain and is quite efficient in dealing with incomplete ambiguous data without strong regularity [23]. It is thus well suited for complicated forecasting problems. As a promising branch of machine learning, deep learning has been reported in literatures [24]. In [25], deep learning is firstly employed in the traffic flow prediction, which has a deep belief network (DBN) at the bottom with a multitask regression layer at the top. However, research only applies DBN in the traditional transportation area but is by far rarely used in EV traffic flow forecasting.

The market mechanism in transmission systems with EV provided FRPs has been studied in several works [26-27], while more work is required for examining and mitigating FRPs provided by EVs in the distribution systems. A hierarchical scheme to utilize EVs to mitigate wind-induced unit ramp cycling operations in the transmission system is established in [26], but the proposed strategy is not carried out in the deregulated market environment. The impact of EV participation in ramp market on power system flexibility is investigated in [27]. Nevertheless, the cooperation of energy market and flexible ramping market, as well as the congestions of the system, are not discussed in this work.

By far, limited efforts have been made to investigate the possibilities of providing FRPs by EVs in the electricity market of the distribution system. Although LMP-based market mechanism is not novel idea in transmission system operation, it has much shorter history to be studied in distribution systems [28] and receives growing attention only in recent years due to the fast development of distribution generators and EVs [29]. As far as FRP provision is concerned, suitable market mechanism in the distribution system is required to providing FRPs properly considering the management of EVs. However, to the best of our knowledge, rare works are conducted to this topic.

Given this background, an EV participated market mechanism in the distribution system considering the provision of FRPs is proposed in this work. The main contributions of this paper are as follows:

1) Deep belief network based model is utilized in the EV traffic flow forecasting, and the availabilities of EV demand for dispatch is estimated by the queuing theory.
2) A novel distribution system based LMP model capable of alleviating congestion and promoting the response of EV charging is modeled to simulate the deregulated market environment. Based on this model, the possible ways of EV participation in the energy market and providing FRPs are explored, with EV operation need and system requirements are considered.
3) An extended ACOPF model is employed to

simultaneously optimize the system cost of providing energy and ramping services, in which the EV aggregators could minimize their costs by participating in energy market and providing FRPs simultaneously. Therefore, EVs' potential to reduce the impacts of load ramps is systematically investigated.

The remainder of this paper is organized as follows: Section II introduces the deep belief network (DBN) based traffic flow forecasting, and potentials of EVs for FRP provision. Section III illustrates EV participated market mechanism considering EV's provision of FRPs. Case studies and discussions are given in Section IV. Section V concludes the paper.

II. Potentials of EVs for FRP Provision

A. Power System Inflexibility and FRPs

With the growing of renewable energy in recent years, maintaining the flexibility becomes a critical problem for the power system operators. This is mainly caused by the uncertain features of renewable energy and changing behaviors of load customers. Inflexibility of power system indicates the difficulty to balance load and supply, which leads to renewable energy curtailments as well as spikes of electricity market prices.

The FRPs are a novel market product to improve the power system flexibility, which introduce new market variables to the existing market model. The utilization of FRPs will reduce power balance violations, potstone the deployment of regulation services, and increase the reliability of the power system.

B. Deep Belief Network Based EV Traffic Flow Forecasting

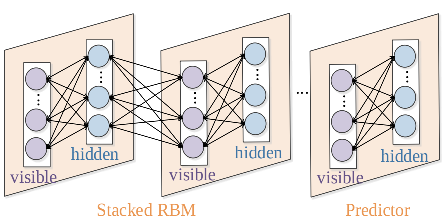

Fig. 1. The DBN framework for forecasting.

It is usually difficult to optimize the weights (neurons) in most kinds of multilayer NNs and limits their forecasting performance. If the initial weights are too large, only poor local minima could be found. If the initial weights are too small, the gradients in the early layers are tiny when training with BP, making it infeasible to obtain the optimal weights in the multilayer NNs [23]. In comparison, the core characteristics of the proposed DBN method lies in that the composition of visible and hidden layers results in a fast-unsupervised process by pre-training a multilayer NN, thus the neurons in the hidden layer could be efficiently optimized to recognize different traffic flow characteristics. Then, the supervised fine-tuning is utilized to adjust the learned features for better prediction.

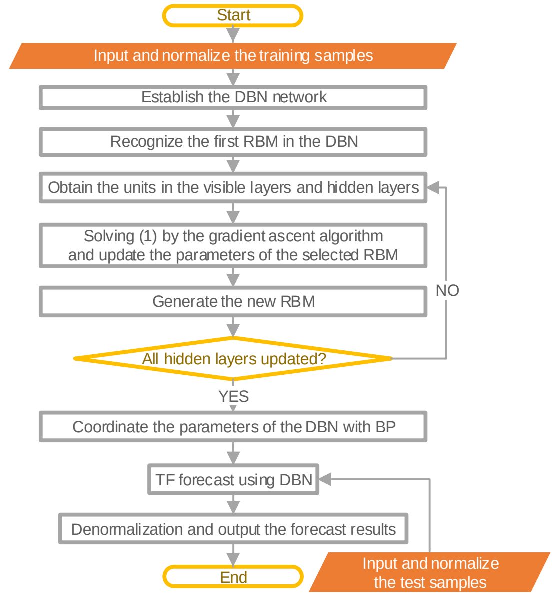

Fig. 2. The flowchart of the proposed DBN framework for forecasting.

DBN consists of restricted Boltzmann machines (RBMs) layer by layer for pre-training and a fine-tuning layer for prediction, as shown in Fig. 1. The historic data is the input and firstly pre-trained by the stacked RBMs in an unsupervised way. The purpose of each RBM is to extract a probability distribution $P(v, h)$ from visible layer v_i to hidden layer h_j to learn the unobservable patterns in the training data, which could be obtained by solving the following optimization according to the Bayesian theory [30].

$$\max \sum_{v\in S}\log P(v,h)=\sum_{v\in S}\log(e^{-E(v,h)}/Z) \tag{1}$$

where S is the training data; Z is the partition function for normalization; and $E(v, h)$ is the energy function assigned to the state of the network:

$$E(v,h)=-\sum_{i=1}^{n_v}a_i v_i-\sum_{j=1}^{n_h}b_j h_j-\sum_{i=1}^{n_v}\sum_{j=1}^{n_h}h_j W_{j,i} v_i \tag{2}$$

in which a_i and b_j are the visible unit offset and the bias weight of the hidden unit, respectively, and $W_{j,i}$ is the matrix of connection weights of visible and hidden units. The size of $W_{j,i}$ is $n_v \times n_h$. All the parameters could be acquired during the solving process of Eq. (1) by stochastic gradient ascent algorithm [31]. The learning of RBMs works well even it is not exactly following the gradient of the log probability (1) of the training traffic flow data [32]. Besides, adding more layers always improves the lower bound on the log probability and ensures the weights are initialized correctly [33]. Therefore, the DBN is very effective to pre-train the weights and makes it an efficient way to reveal low-dimensional, nonlinear structure of the traffic flows to achieve higher forecasting performance than other technologies.

In the final stage of the whole network, the fine-tuning is utilized as the predictor to coordinate the parameters of the DBN, which could be solved by the well-known back propagation (BP) in a supervised manner. As a summary, the flowchart of the proposed DBN method is shown in Fig. 2.

To assess the effectiveness of the DBN method, the indices of mean absolute error (MAE), mean absolute percentage error

(MAPE) and root mean square error (RMSE) could be used, which are defined as:

$$\text{MAE} = (1/N)\sum_{i=1}^{N} | TF_i^a - TF_i^f | \tag{3}$$

$$\text{MAPE} = (1/N)\sum_{i=1}^{N} (| TF_i^a - TF_i^f | /((\sum_{i=1}^{N} TF_i^a)/N)) \times 100\% \tag{4}$$

$$\text{RMSE} = \sqrt{(1/N)\sum_{i=1}^{N} | TF_i^a - TF_i^f |^2} \tag{5}$$

where N is the training samples number, TF_i^a is the true traffic flow, and TF_i^f is the forecasted traffic flow.

C. EV Availability Estimation

Fast-start power system components such as gas plants, pumped hydro, fly wheel or compressed air could provide FRPs to the system. However, most of such methods are available but too expensive for widespread applications. Nowadays, some loads, such as loads in households for temperature control, are flexible and dispatchable. It is possible for these dispatchable loads to react to energy market signals to reduce their cost. Moreover, batteries of EVs are controllable to achieve smart charging and have possibilities to respond to energy market signals. On the other hand, net load ramps exist in the distribution system [34], which could lead the distribution system into balance violations and price spikes if not properly handled. Compared to the existing EV participated market mechanism, the EV abilities of FRP provision to eliminate the impacts of load ramps, is taken into the consideration in the proposed model due to their good controllability and fast responsive characteristics.

The dispatchable demand in the EV aggregator is dynamic and highly dependent on the traffic flow passing by the EV aggregator, the temporal distribution of which could be predicted by the EV aggregator operators. The EV's charging in the EV aggregator is a probabilistic queuing process, and the arrival EV number n of each time step follows a Poisson process:

$$P(n) = e^{-\lambda}(\lambda^n/(n!)) \qquad n=0,1,2... \tag{6}$$

where λ is the average arrival EV number at each time step. The charging duration t_c follows a negative exponential distribution.

$$f(t_c) = \mu e^{-\mu t_c} \tag{7}$$

where μ is average number of EVs that complete charging and leave the EV aggregator at each time step. According to the queuing theory, the dispatchable EV number is $N^{\text{avi}}=\lambda/\mu$. In practice, some EV users do not have willingness to be ordered to adjust their demand or react to economic signals even if subsidy incentives exist. Therefore, υ, a tolerant coefficient less than 1, is introduced to solve this situation in the proposed approach, and the available EV power $P^{\text{FL,avi}}$ is

$$P^{\text{FL,avi}} = \upsilon N^{\text{avi}} p_r^{\text{EV}} \tag{8}$$

where p_r^{EV} is the rated power of chargers in the EV aggregator, and υ guarantees that the system requirement could be met when only a portion of EVs are willing to adjust their demand.

III. EV Participated Market Mechanism

A. Motivations for the Market Mechanism Design

Given the increasing penetration of distributed energy resources in distribution networks, consumers have more flexible distributed generation and storage resources and have the potential to become prosumers, i.e., producers and consumers. In other words, peer-to-peer trading and aggregated energy trading in a distribution market will be emerging and transactive energy will be a new paradigm of energy supply. In the meantime, if more energy demand can be satisfied in the distribution market, transactions at the transmission level market may become less. Recently, this transition from a transmission level market to a distribution level market has been put forward by many government relevant reports such as [35-36].

The concept of LMP is usually used in transmission systems or distribution systems with distribution generators. The LMP-based distribution market has attracted attention from the research scholars, and we have found research works on this topic, such as [36-41]. The designed distribution system market architecture in this work has many advantages in the operation of the distribution system, including but not limited to congestion alleviation and ramp reduction. For example, the LMP-based mechanism could be used in distribution system to allocate the loss and remunerate the DG more efficiently [42], to identify and recover long-run investment costs [43], to allocate loss and emission reduction [40], or to facilitate PV penetration [41]. Given that dispatchable loads such as EVs widely existed in the distribution system, a novel LMP-based distribution market mechanism is proposed in this work to encourage the dispatchable loads such as EVs to react to economic signals.

Meanwhile, net load ramps exist extensively in the distribution system, which could drive the distribution system into balance violations and power flow congestions if not properly handled. Traditional studies focus on direct control of loads, transformers, or distribution generators to avoid the drawbacks of congestions and ramps. However, it is not very effective to apply such control methods because users do not have willingness to be ordered to adjust their demand. The growing challenges of maintaining electricity sully-demand balance in distribution system lead to higher requirement for ramping products in distribution level [44-45].

Therefore, the concept of FRP price is introduced to ensure the net load ramps are met reliably and economically with true marginal costs, and the established market mechanism is based of locational marginal pricing (LMP) of energy and marginal pricing of FRPs. To calculate the marginal pricing of energy and FRPs with the consideration of congestions, power losses, and ramping requirements, an extended alternative current optimal power flow (ACOPF) is employed. The FRPs will reserve the ramp capacity to maintain the power balance of the system, and the ramp capacity need is incorporated into the traditional ACOPF based Locational marginal pricing (LMP) model.

In the distribution system, EV loads of aggregators, and some other flexible loads, are considered dispatchable, and are stated as follows:

$$P_{m,t}^{\mathrm{L}}=\begin{cases}P_{m,t}^{\mathrm{noEA}},\ \forall m\in\Omega^{\mathrm{noEA}}\\ P_{i,t},\ \forall m\in(\Omega^{\mathrm{B}}-\Omega^{\mathrm{noEA}}),\forall i\in\Omega^{\mathrm{EA}}\end{cases}\tag{9}$$

$$P_{m,t}^{\mathrm{noEA}}=\begin{cases}P_{m,t}^{\mathrm{U}}+P_{m,t}^{\mathrm{D}},\forall m\in\Omega^{\mathrm{D}}\\ P_{m,t}^{\mathrm{U}},\ \forall m\in(\Omega^{\mathrm{noEA}}\text{-}\Omega^{\mathrm{D}})\end{cases}\tag{10}$$

$$P_{i,t}=P_{i,t}^{\mathrm{U}}+P_{i,t}^{\mathrm{FL}},\forall i\in\Omega^{\mathrm{EA}}\tag{11}$$

Eq. (9) assumes that there are no other loads except EV aggregator demand on nodes where new EV aggregators are located. As shown in Eq. (10) and (11), parts of loads are dispatchable.

B. Objective Function

Prices are essentially important for the development of EVs, which leads to strong willingness of EVs to participant this market to obtained profits and reduce their charging cost. Considering the participation of the available EV power, the objective of the extended ACOPF model is to minimize the overall electricity system cost, as well as the total supplying cost for the FRPs in the distribution system.

$$\begin{aligned}\min\ F=\sum_{t\in\Omega^{\mathrm{T}}}D_t[\sum_{m\in\Omega^{\mathrm{S}}}p_{m,t}^{\mathrm{L}}P_{m,t}^{\mathrm{S}}-\sum_{m\in\Omega^{\mathrm{noCS}}}p_{m,t}^{\mathrm{L}}P_{m,t}^{\mathrm{noEA}}-\sum_{i\in\Omega^{\mathrm{CS}}}p_{i,t}^{\mathrm{L}}P_{i,t}]\\ +D_t\sum_{t\in\Omega^{\mathrm{T}}}\sum_{i\in\Omega^{\mathrm{EA}}}\pi_{i,t}^{\mathrm{raup}}c_{i,t}^{\mathrm{raup}}R_{i,t}^{\mathrm{raup}}\end{aligned}\tag{12}$$

The first part in (12) denotes the electricity purchasing cost from the substations connecting to the upper-level transmission system. The second and third parts in (12) denote the incomes of selling energy to the EV loads and other flexible loads, and model them as negative real power injections with associated negative costs, while the negative cost is equivalent to benefits for consumption. The last part in (12) denotes the cost for EVs to provide the ramp service. The ramping down is ignored and only the ramping up is focused without loss of generality.

C. Network Constraints

$$U_m^{\min}\le U_{m,t}\le U_m^{\max},\ \forall m\in\Omega^{\mathrm{B}}\tag{13}$$

$$P_{m,t}^{\mathrm{S}}-P_{m,t}^{\mathrm{L}}-U_{m,t}\sum_{m,n\in\Omega^{\mathrm{B}}}U_{n,t}(G_{mn}\cos\theta_{mn,t}+B_{mn}\sin\theta_{mn,t})=0\quad\forall m,n\in\Omega^{\mathrm{B}}\tag{14}$$

$$Q_{m,t}^{\mathrm{S}}-Q_{m,t}^{\mathrm{L}}-U_{m,t}\sum_{m,n\in\Omega^{\mathrm{B}}}U_{n,t}(G_{mn}\sin\theta_{mn,t}-B_{mn}\cos\theta_{mn,t})=0\quad\forall m,n\in\Omega^{\mathrm{B}}\tag{15}$$

$$(P_{m,t}^{\mathrm{S}})^2+(Q_{m,t}^{\mathrm{S}})^2\le(S_m)^2\quad\forall m\in\Omega^{\mathrm{S}}\tag{16}$$

$$P_{mn,t}=U_{m,t}^2G_{mn}-U_{m,t}U_{n,t}(G_{mn}\cos\theta_{mn,t}+B_{mn}\sin\theta_{mn,t})\quad\forall m,n\in\Omega^{\mathrm{B}}\tag{17}$$

$$Q_{mn,t}=-U_{m,t}^2B_{mn}-U_{m,t}U_{n,t}(G_{mn}\sin\theta_{mn,t}-B_{mn}\cos\theta_{mn,t})\quad\forall m,n\in\Omega^{\mathrm{B}}\tag{18}$$

$$P_{mn,t}^2+Q_{mn,t}^2\le(S_{mn}^{\max})^2,\forall m,n\in\Omega^{\mathrm{B}}\tag{19}$$

$$P_{m,t}^{\mathrm{D,min}}\le P_{m,t}^{\mathrm{D}}\le P_{m,t}^{\mathrm{D,max}},\forall m\in\Omega^{\mathrm{F}}\tag{20}$$

$$P_{i,t}^{\mathrm{FL,min}}\le P_{i,t}^{\mathrm{FL}}\le P_{i,t}^{\mathrm{FL,max}},\forall i\in\Omega^{\mathrm{EA}}\tag{21}$$

The network constraints contain the active and reactive power flow limits of each branch, voltage magnitude and phase angle limits of each bus. Inequality (13) is the voltage magnitude constraint. Eq. (14) and (15) denote the typical AC power flow equality constraints for each bus, which mean that the sum of power flowing into this node is equal to the sum of power flowing out of that node [46]. This ensures a balanced steady operation state of the distribution system by nonlinear equations of nodal power and nodal voltage phasors [47]-[48]. Eq. (16) compactly gives the capacity constraints for substations. Meanwhile, the active and reactive power of distribution system feeders is determined by the Eq. (17) - (18). The transferred electricity power of the distribution system feeders should not exceed their designed transfer capacities, which are constrained by Eq. (19). Eq. (20) shows the upper and lower limits of dispatchable load on nodes where no EV aggregators are located. Eq. (21) gives the upper and lower limits of the dispatchable load of EV aggregator *i*.

D. Ramp Capacity Constraints

$$\mathrm{e}_{i,t}^{\mathrm{raup}}=D_tR_{i,t}^{\mathrm{raup}}\tag{22}$$

$$e_{i,t}^{\mathrm{raup}}\le D_tP_i^{\max},\ \forall i\in\Omega^{\mathrm{EA}}\tag{23}$$

$$R_{i,t}^{\mathrm{raup}}\le\min(R_{i,t}^{\mathrm{raup,max}},\Delta_i),\forall i\in\Omega^{\mathrm{EA}}\tag{24}$$

$$\sum_{i\in\Omega^k}R_{i,t}^{\mathrm{raup}}\ge R_t^k,k=1,\ldots,K\tag{25}$$

$$P_{i,t},\ \mathrm{e}_{t,i}^{\mathrm{raup}},R_{i,t}^{\mathrm{raup}}\ge0\tag{26}$$

In this work, EVs provide ramp capacity to maintain the system power balance in the form of FRPs and receive rewards of giving such kind of service. On the other hand, a part of EV energy is reserved for FRP provisions. Eq. (22) states the relationship of ramp power and ramp capacity. Inequality (23) denotes the ramp capacity does not exceed the maximum available energy. (24) indicates that the ramp power provided by the EV aggregator are limited by the maximum ramp rate as well as their physical ramp rates Δ_i. In constraint (25), the FRP requirements are defined as a set of *K* fixed zonal quantities. Let Ω^{k} be the set of EV aggregators in zone *k* and R_t^k be the FRP requirement for zone *k*. (25) requires that the sum of the ramp power should meet the requirements within each zone *k*, and this constraint ensures the expected variability could be met. Eq. (26) requires the active power EV aggregator *i* offered to EVs, the ramp capacity provided by EVs, as well as ramp power should be positive. All the constraints should be satisfied to make sure that EVs have the abilities to participate the ramp market.

E. EV Operation Constraints

$$\mathrm{Soc}_{i,t}=\mathrm{Soc}_{i,t-1}+\eta_i^{\mathrm{chg}}P_{i,t}D_t,\ \forall i\in\Omega^{\mathrm{EA}}\tag{27}$$

$$\mathrm{e}_{i,t}^{raup}\le\mathrm{Soc}_{i,t}-\mathrm{Soc}_i^{\min},\ \forall i\in\Omega^{\mathrm{EA}}\tag{28}$$

$$\mathrm{Soc}_i^{\min}\le\mathrm{Soc}_{i,t}\le\mathrm{Soc}_i^{\max}\ \ \forall i\in\Omega^{\mathrm{EA}}\tag{29}$$

$$\mathrm{Soc}_{i,t=|T|}=\mathrm{Soc}_i^{req}\ \ \forall i\in\Omega^{\mathrm{EA}}\tag{30}$$

Equations (27) - (30) state the energy state-of-charge (Soc) limits of EV aggregators. The change of Soc between two neighboring time intervals is described in (27), which is related to its present charging power. (28) indicates the ramp capacity of EV aggregator *i* for upward FRP in period *t* should not be more than the available energy stored in the batteries of EVs.

(29) demonstrates the minimal and maximal stored energy constraints. (30) guarantees the Soc in the end of the time period should be equal to the required Soc, which indicates the electric energy required for the travelling consumption could be satisfied.

F. Prices of Energy and FRPs

In this optimization model, network parameters, power flow limits and output limits are known data for the optimization. Some required data such as load demand and traffic flow levels are forecasted by the market operators to solve this distribution system market optimization model.

In this model, LMP of energy is defined as the marginal cost for meeting the increment of demand for the specific location, which is also defined as the partial derivative of Lagrange function with respect to an incremental load change and can be obtained by solving the proposed market mechanism optimization [49]. Dispatchable loads such as EVs are required to have biddings on the FRPs, and the FRPs are priced at the marginal values of the FRP requirements, which is calculated as the dual variable of the ramp capacity constraint (as shown in Eq. (25)) [27]. Similarly, the marginal pricing for FRPs in a zone is the incremental cost for meeting an additional megawatt of the FRPs in this zone. By solving the proposed ACOPF model, LMPs and FRP prices will be obtained.

G. Scenario-based Approach for System Uncertainties

Various uncertainties affect the operation of the distribution system, which should be properly treated to minimize risk, avoid accidental losses and minimize running problems. Scenario-based approach could address such kind of problems and is used in this work to deal with uncertainties involved in the proposed model.

Load demand levels, traffic flow levels, penetration levels of EVs, and penetration levels of renewables are the four uncertainties considered in this paper. And the four uncertainties are stated by the vector as

$$\boldsymbol{\Phi}_s = [\boldsymbol{P}_s^{\mathrm{D}}, \boldsymbol{TF}_s, \beta_s^{\mathrm{EV}}, \gamma_s^{\mathrm{RE}}] \quad \forall s \in \Omega^{\mathrm{s}} \tag{31}$$

where $\boldsymbol{\Phi}_s$ represents scenario s; $\boldsymbol{P}_s^{\mathrm{D}}$ is the load demand vector in scenario k; $\boldsymbol{TF}_s$ is the traffic flow vector (including traffic flow passing by all nodes) in scenario k; β_s^{EV} and γ_s^{RE} are the penetration levels of EVs and renewables in scenario k, respectively.

The traffic flow passing by the candidate EV aggregators and load demands are forecasted as an important precondition for the EV aggregator optimization. Deviation strategy [50] is utilized to the forecasted values to generate related uncertainty scenarios. For instance, if 2 scenarios should be generated for traffic flow, the specific results could be (1+a%)×forecasted traffic flow and (1-a%)×forecasted traffic flow respectively, where a% is the bias added to the forecasted results. Meanwhile, the penetration levels of EVs and renewables are affected by many aspects such as subsidy policies and technology developments, which could hardly be forecasted by historical data. Scenarios for such kinds of uncertainties are directly predefined.

IV. Case Study and Discussions

A. Test System and Experiment Data Description

As shown in Fig. 3, an 11-kV 36-node system is used to show the effectiveness of the proposed model. This 11-kV 36-node system represents a typical UK distribution system, the load of which is proportional (0.01%) to that of the UK [51]. The traffic flow on the roads is from the official website of Highways England [52-53]. Fig. 3 is the distribution network of the test system. As shown by the Lateral 1-3 in Fig. 3, the loads are divided into 3 categories: commercial, industrial, and residential, while the Lateral 4 composites load of the 3 kinds. The normalized load patterns of the 3 kinds of loads are shown in Fig. 4.

Three EV aggregators are located at node 33, 34 and 37. Two wind power turbines are located at node 2 and node 5. Two substations are located at node 1 and node 6.

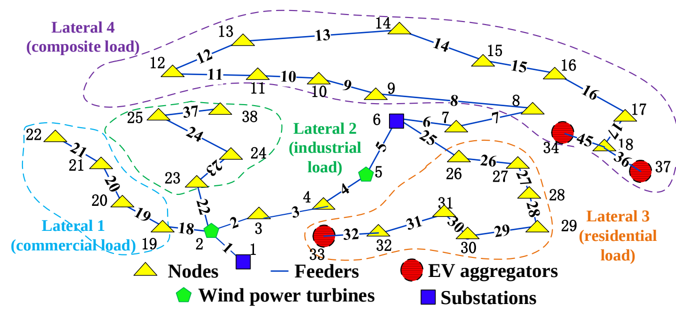

Fig. 3. The 36-bus distribution system

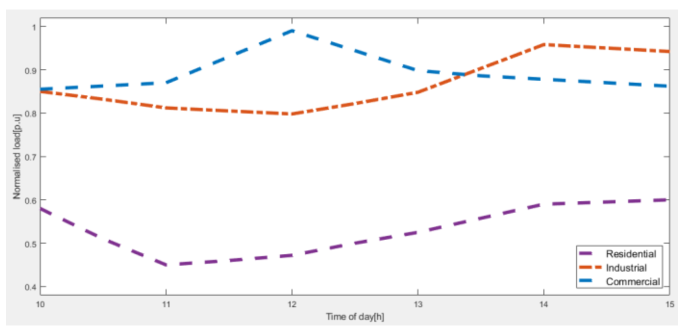

Fig. 4. Normalized load patterns of different load categories.

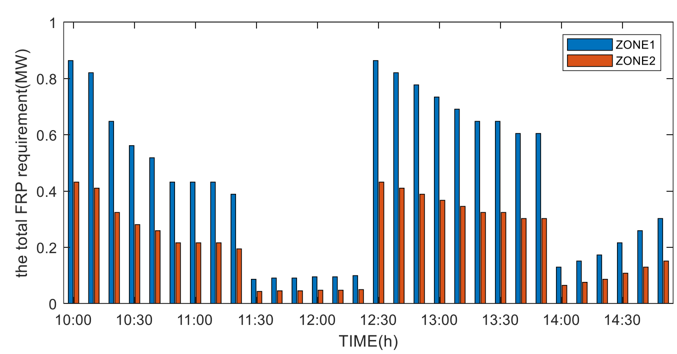

Fig. 5. The total FRP requirement curve

Loads in node 13, 20, and 23 are set to be controllable. Loads of EV aggregators are also assumed dispatchable and be able to provide FRPs. On nodes with both flexible and inflexible loads, the proportion of its inflexible loads and the maximum of its flexible loads are 70% and 30%, respectively. The substation

(substation 1 on node 1) offers and controllable load bids are listed in Table I. The substation 2 on node 6 is assumed to provide FRPs. The marginal cost of ramp service for EV aggregators and substation 2 is shown in Table II. The system is divided into 2 zones. The substation 2, EV aggregator 1 and EV aggregator 3 are in both zone 1 and zone 2. EV aggregator 2 only belongs to zone 1. The total FRP requirements of 2 zones are shown as Fig. 5. The required SOC value for the EV operation constraint is set to 92.2%.

TABLE I

THE SS1 OFFERS AND LOAD/EA BIDS (US$/MWh)

SS1	EA1	EA2	EA3	Node13	Node20	Node23
100	150	150	150	120	120	120

SS1: Substation 1; EA: EV aggregator

TABLE II

THE MARGINAL COST OF RAMP SERVICE FOR EV AGGREGATOR AND SUBSTATION (US$/MW)

	Locations	Cost	Zone
EV aggregator 1	node 33	700	1, 2
EV aggregator 2	node 34	500	1
EV aggregator 3	node 37	400	1, 2
Substation 2	node 6	300	1, 2

The simulation results are obtained on a laptop computer with 8 GB RAM and an Intel(R) Core(TM) i5-7200U CPU clocked at 2.50GHz. The EV participated market model is efficiently solved by the interior point algorithm [54].

B. Forecast Results Analysis

The traffic flow passing by the EV aggregators has first to be forecasted as an important precondition for the market participation of EVs. The data for DBN based forecasting is obtained in [52-53] in 10-min intervals. Table III firstly verifies the performance of the DBN based traffic flow forecasting on node 33 and 37 compared with the Back Propagation Neural Network (BPNN), Support Vector Machine (SVM), Auto-Regressive and Moving Average Model (ARMA), and Morlet Wavelet Neural Network (MWNN). The DBN method has lower MAE, MAPE and RMSE values than other methods, which indicates that the DBN method has a better performance in forecasting the traffic flows. Fig. 6 demonstrates the forecasting curves of different methods on node 37. It could be found that the forecasted result by the DBN method is closest to the actual data among the 4 methods, which verifies its good performance. After the performance of the DBN is verified, the traffic flow curve for the market participation is forecasted and fed to the proposed model.

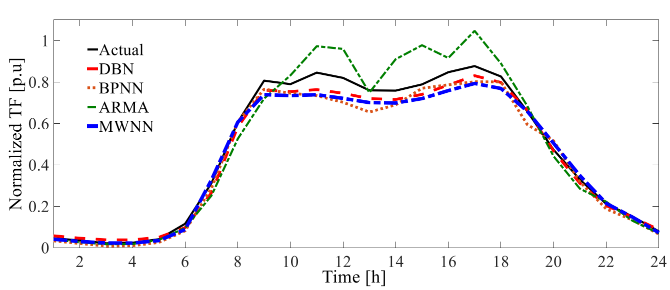

Fig. 6. Forecasting results by different methods on node 37.

TABLE III

TRAFFIC FLOW FORECASTING ERROR COMPARISON AT NODE 33 AND 37

Location	Error	BPNN	SVM	ARMA	MWNN	**DBN**
Node 37	MAE	114.63	107.48	122.07	122.72	**106.81**
	RMSE	151.21	150.83	165.58	162.69	**144.61**
	MAPE(%)	11.88	11.14	12.65	12.72	**11.07**
Node 33	MAE	53.89	39.61	45.18	52.09	**37.29**
	RMSE	93.70	54.64	71.86	68.12	**48.47**
	MAPE(%)	14.45	10.62	12.11	13.96	**10.00**

C. Ramp Power and Prices Results

Fig. 7 to Fig. 9 depict the ramp power of each aggregator, the FRP price of each aggregator, and the FRP price in zone 1 and zone 2, respectively. And the computation time of this case is 8.899 seconds. It can be found in Fig. 7 that the EV aggregators provide relatively more ramp power during the time period 10:00-11:20 and 12:30-13:50, which means more EV power is dispatched as FRPs during these 2 time periods. Meanwhile, as shown in Fig. 8 and Fig. 9, the FRP price of each aggregator, as well as the FRP prices in zone 1 and zone 2, are higher during the mentioned 2 time periods. This is because that when more ramp power is needed to maintain the balance of the system, the EVs with higher ramping cost are dispatched to provide the ramping service, which leads to a higher FRP price. On the other hand, the higher FRP price will give more rewards to the EVs. Therefore, the proposed FRP market-based mechanism will incentive EVs to provide the ramping service with higher rewards, while reducing their overall cost and benefiting the EV owners at the same time. From Fig.9, during the time period 10:50-12:40 and 14:00-15:00, the FRP price in zone 2 is zero. It is because when the FRP requirement within zone 1 is satisfied, the available ramp power in zone 2 exceeds the FRP requirement within zone 2.

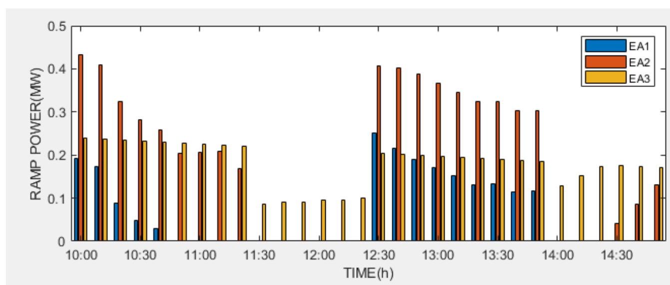

Fig. 7. The ramp power of each EV aggregator.

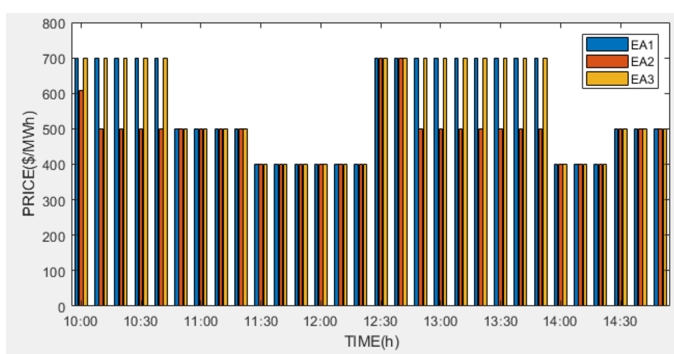

Fig. 8. The FRP price of each EV aggregator.

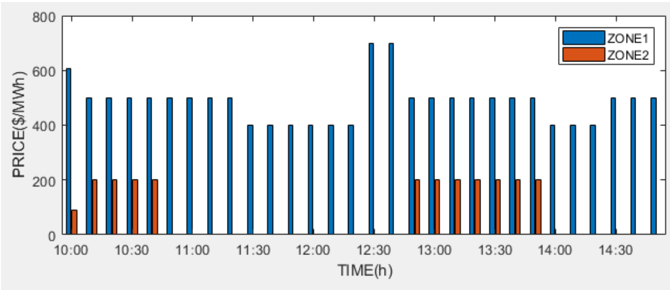

Fig. 9. The FRP prices in zone 1 and zone 2.

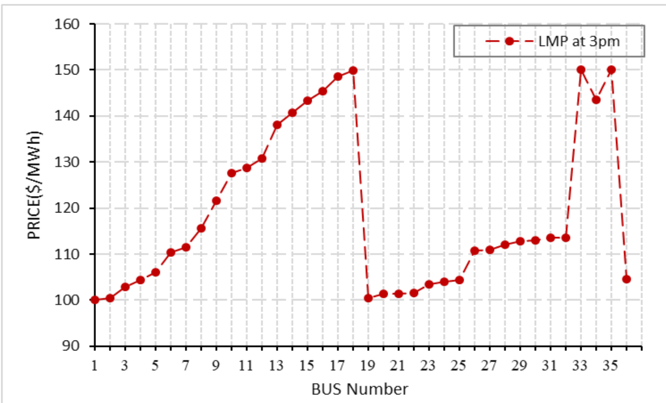

Fig. 10. The LMP of each node at 3pm.

Meanwhile, Fig. 10 gives the LMPs of each bus at the time of 3pm, which range from 100 \$/MWh to 150 \$/MWh. The different LMPs indicate the variation of purchasing electricity energy for the customers, which could be caused by the congestions, power losses, et al.

The average Soc of an EV in the EV aggregator on node 33 is illustrated in Fig. 11. It can be seen that the required Soc is satisfied in the end of the time period. Furthermore, in Fig. 12, Fig. 13 and Fig. 14, results for 24 hours are given. According to the forecasting results of the traffic flow curve, EV aggregators cannot offer FRP service in certain period time of a day (i.e. from 0 a.m. to 6 a.m.), which is also demonstrated in Fig. 12 and Fig. 13. The SOC curve of EV aggregator throughout the 24 hour is depicted in Fig. 14, which is different from the SOC of a single EV. This is because the SOC curve of the aggregator is not only determined by the charging power, but also impacted significantly by the arrivals of EVs with small SOC and the departments of EVs with fully charged batteries (large SOC) in different time of a day. For example, if a large number of EVs with small SOC arrived at the EV aggregator simultaneously, the SOC of this aggregator will decrease.

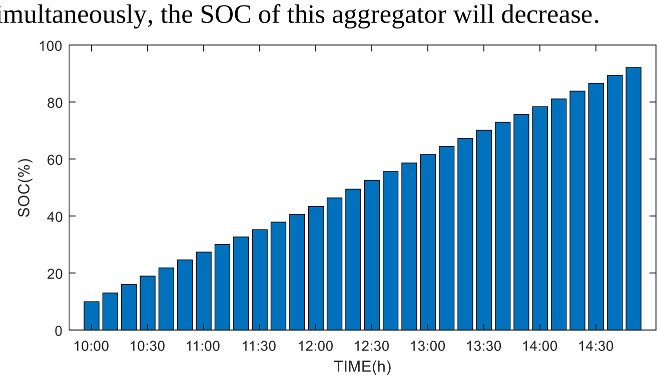

Fig. 11. The SOC curve of an EV in the EV aggregator on node 33.

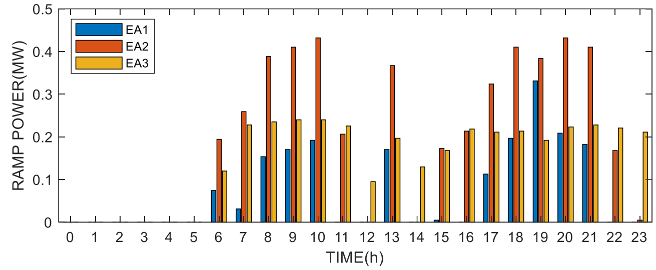

Fig. 12. The ramp power of each EV aggregator in 24 hours.

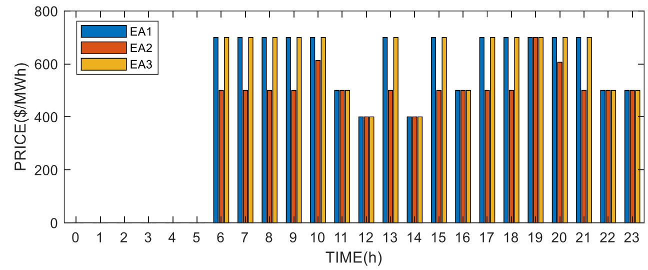

Fig. 13. The FRP price of each EV aggregator in 24 hours.

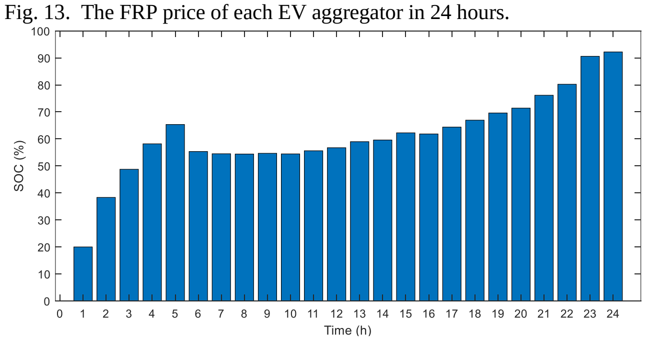

Fig. 14. The SOC of the EV aggregator on node 33.

D. *Coordination of EVs and Other FRP Providers*

Because there usually exist different kinds of dispatchable components in the distribution system, the coordination of EVs and other FRP provides should be considered. For example, the substations also have abilities to give ramping services, and the coordination of EV aggregators and substations to provide FRPs is studied in this part. There are several reasons for the coordination of substations and EV aggregators. Firstly, the batteries of EVs may not have enough capacities for the requirements of the system to maintain the power balance. Secondly, the FRP provisions of substations will give the system more flexibilities for the ramping service. As shown in Fig. 15, substation is the only source to provide the ramp power during the time period of 11:30-12:20, which indicates that EVs do not need to be dispatched as FRP providers. Fig. 16 shows the FRP price of each EV aggregator and the substation, which are priced at the marginal values of the FRP requirements, and different zones have different requirements. Noticing in Table II that the substation, EV1 and EV3 belong to zone 1&2, while EV2 only belongs to zone 2, it can be understood that the prices of FRP are the same for substation, EV1 and EV3, but the FRP price for EV2 is different with the others. The FRP prices in zone 2, as depicted in Fig. 17, also demonstrate that the participation of substations will reduce the FRP price during some time periods of the day. This is because that the substation has lower cost to provide ramp services. However, due to the capacity limitations of substations, in most time of the studied period, EVs and substations will provide FRPs simultaneously. Obviously, the participation of EVs for ramp service will enhance the system flexibility and gives more options to maintain the system power balance.

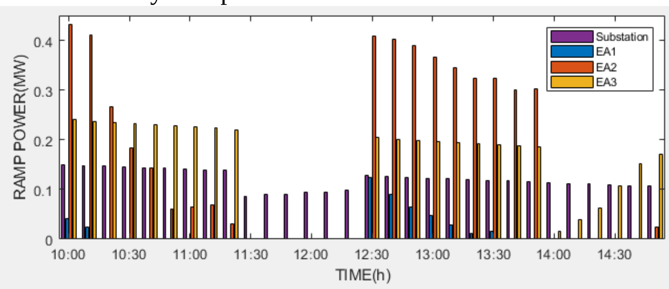

Fig. 15. The ramp power of EV aggregator and the substation.

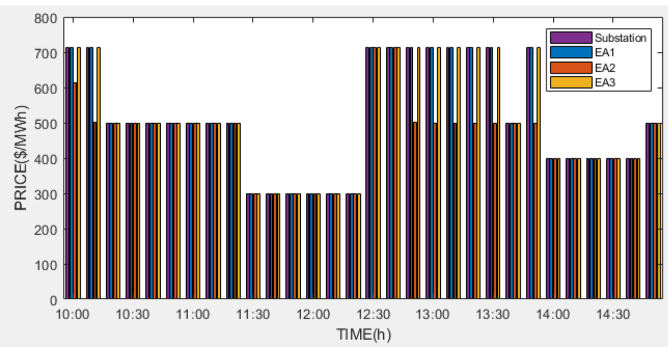

Fig. 16. The FRP price of each EV aggregator and the substation.

E. Sensitivity Test with Different Scenarios

Based on the forecasted results, 2 scenarios, 0.9×forecasted value and 1.1×forecasted value, are constructed for the load levels and traffic flow levels respectively. Scenarios for the penetration levels of EVs and renewables are directly assumed, setting the penetration values with 0.2 and 0.4 (proportions in all vehicles or total power). For example, the vector [1.1, 0.9, 0.4, 0.2] stands for the scenario that the load demand is 1.1 times of the forecasted value, traffic flow level is 0.9 times of the forecasted value, the penetration of EV is 0.4 and the penetration of renewables is 0.2. The detailed scenarios description is shown in Table IV. Besides, the occurrence probability is set to be the same for each scenario. Therefore, 16 scenarios are set up.

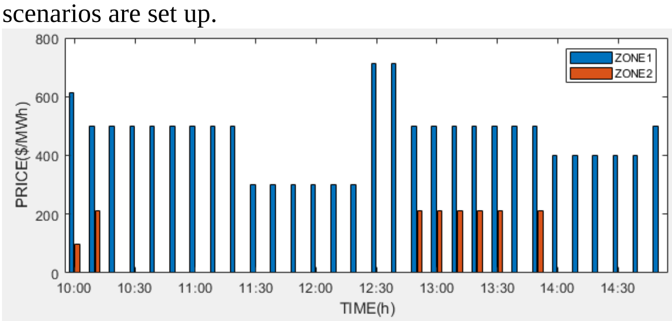

Fig. 17. The FRP price in zone 1 and zone 2 with substations.

TABLE IV

SETTINGS OF SCENARIOS

No	Scenario descriptions	No	Scenario descriptions	No	Scenario descriptions
S1	1.1,0.9,0.2,0.2	S7	1.1,1.1,0.4,0.2	S13	0.9,0.9,0.2,0.2
S2	1.1,0.9,0.2,0.4	S8	1.1,1.1,0.4,0.4	S14	0.9,0.9,0.2,0.4
S3	1.1,0.9,0.4,0.2	S9	0.9,1.1,0.2,0.2	S15	0.9,0.9,0.4,0.2
S4	1.1,0.9,0.4,0.4	S10	0.9,1.1,0.2,0.4	S16	0.9,0.9,0.4,0.4
S5	1.1,1.1,0.2,0.2	S11	0.9,1.1,0.4,0.2		
S6	1.1,1.1,0.2,0.4	S12	0.9,1.1,0.4,0.4		

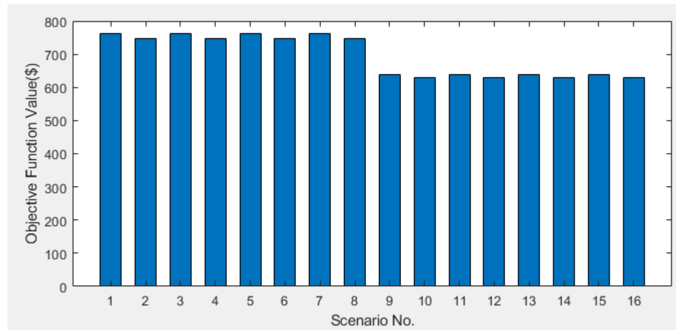

Fig. 18. The objective function values of different scenarios.

The objective function values of different scenarios are depicted in Fig. 18. It can be found that the objective values are sensitive to the scenario settings, which verifies that the objective values change in different scenarios. Obviously, the uncertainties impact the optimization results significantly and should be properly handled by the market operators.

The relationship between each uncertainty parameters to the objective value can be found from Fig.19 - Fig.22, and the effect of load levels, traffic flow, EV penetration and renewable penetration are stated as follows:

1) The effect of load levels: Fig.19 illustrates the objective function values of different scenarios (red bar graph) when 0.7×forecasted value and 1.3×forecasted value are constructed for the load levels and other uncertainty parameters (traffic flow levels, the penetration levels of renewables and EV) are not changed as Table IV shows. Blue bar graph in Fig.19 is the same as Fig.18. It can be found that the objective function value increases as load demand increases. In other words, the load levels have negative impacts on the objective function value.

2) The effect of traffic flow: Similarly, in Fig.20, red bar graph depicts the objective function values of different scenarios when 0.7×forecasted value and 1.3×forecasted value, are constructed for the traffic flow levels and other uncertainty parameters are the same as Table IV shows. It can be noticed that the decreasing of traffic flow leads to the increasing of the objective function value.

3) The effect of EV penetration: The penetration values with 0.2 and 0.4 for the penetration levels of EVs are replaced of 0.8 and 0.6 in Fig.21. Compared to other impact factors, the EV penetration has a minor effect on the value of objective function.

4) The effect of renewable penetration: The values for the penetration levels of renewables with 0.2 and 0.4 are replaced of 0.8 and 0.6 in Fig.22. It can be observed that the increase of renewables penetration rate will decrease the objective function value.

Overall, the load levels have more remarkable impact than other parameters on the objective function value.

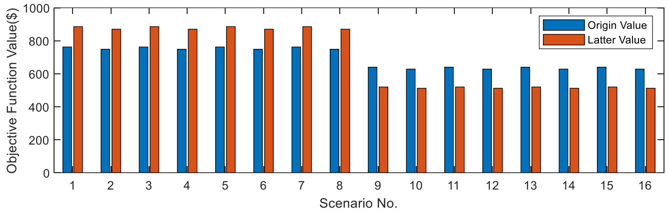

Fig. 19. The objective function values of different scenarios when load levels are changed

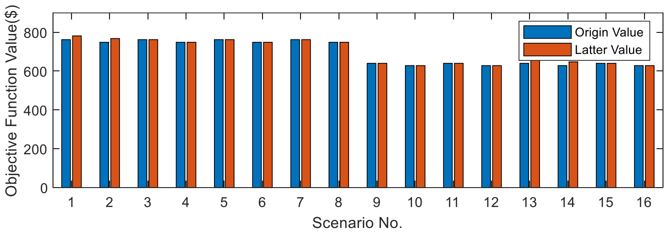

Fig. 20. The objective function values of different scenarios when traffic flow levels are changed

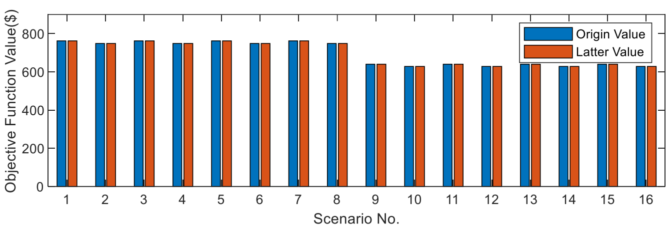

Fig. 21. The objective function values of different scenarios when the penetration levels of EVs are changed

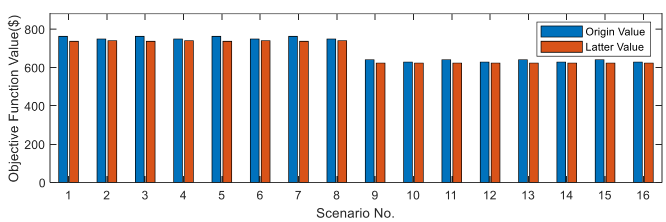

Fig. 22. The objective function values of different scenarios when the penetration levels of renewables are changed

V. Conclusions

A novel EV participated LMP model considering FRP provision in the distribution system is set up in this work to realistically explore the potentials of dispatching EV demands.

The effectiveness of proposed electricity market model with EV involved is proved for its immediate and far-reaching significance to promote the development of EVs. The limitations of this work include the lack of integration of many other ancillary services such as reserve and regulations, or the utilization of stochastic optimization to cope with uncertainties, which will be studied in the future work.

References

[1] A. Hajimiragha, C. A. Canizares, M. W. Fowler, and A. Elkamel, “Optimal transition to plug-in hybrid EVs in Ontario, Canada, considering the electricity-grid limitations,” *IEEE Trans. Ind. Electron.*, vol. 57, no. 2, pp. 690-701, Feb. 2010.

[2] C. Pang, P. Dutta and M. Kezunovic, "BEVs/PHEVs as Dispersed Energy Storage for V2B Uses in the Smart Grid," in *IEEE Transactions on Smart Grid*, vol. 3, no. 1, pp. 473-482, March 2012.

[3] Xi Lu, K. W. Chan, Shiwei Xia, Xian Zhang, Guibin Wang, Furong Li, "A Model to Mitigate Forecast Uncertainties in Distribution Systems Using the Temporal Flexibility of Electric Vehicle Aggregators," in *IEEE Transactions on Power Systems*, vol. 35, no. 3, pp. 2212-2221, May 2020.

[4] J. M. Foster and M. C. Caramanis, "Optimal Power Market Participation of Plug-In Electric Vehicles Pooled by Distribution Feeder," in *IEEE Transactions on Power Systems*, vol. 28, no. 3, pp. 2065-2076, Aug. 2013.

[5] S. Li, M. Brocanelli, W. Zhang and X. Wang, "Integrated Power Management of Data Centers and Electric Vehicles for Energy and Regulation Market Participation," in *IEEE Transactions on Smart Grid*, vol. 5, no. 5, pp. 2283-2294, Sept. 2014.

[6] M. R. Sarker, Y. Dvorkin and M. A. Ortega-Vazquez, "Optimal Participation of an Electric Vehicle Aggregator in Day-Ahead Energy and Reserve Markets," in *IEEE Transactions on Power Systems*, vol. 31, no. 5, pp. 3506-3515, Sept. 2016.

[7] N. Navid and G. Rosenwald, "Market Solutions for Managing Ramp Flexibility With High Penetration of Renewable Resource," in *IEEE Transactions on Sustainable Energy*, vol. 3, no. 4, pp. 784-790, Oct. 2012.

[8] Q. Wang and B. Hodge, "Enhancing Power System Operational Flexibility With Flexible Ramping Products: A Review," in *IEEE Transactions on Industrial Informatics*, vol. 13, no. 4, pp. 1652-1664, Aug. 2017.

[9] CAISO, “Business requirements specification: Flexible ramping product,” version 1.2, Mar. 2013.

[10] L. Xu, D. Tretheway, “Flexible ramping products: Draft final proposal,” California ISO, Folsom, CA, USA, pp. 1–51, Apr. 2012.

[11] N. Navid and G. Rosenwald, “Ramp capability product design for MISO markets,” Midwest Independ. Syst. Oper., Carmel, IN, USA, pp. 1–67, Jul. 2013.

[12] C. Wu, G. Hug and S. Kar, "Risk-Limiting Economic Dispatch for Electricity Markets with Flexible Ramping Products," in *IEEE Transactions on Power Systems*, vol. 31, no. 3, pp. 1990-2003, May 2016.

[13] B. Wang and B. F. Hobbs, "Real-Time Markets for Flexiramp: A Stochastic Unit Commitment-Based Analysis," in *IEEE Transactions on Power Systems*, vol. 31, no. 2, pp. 846-860, March 2016.

[14] M. Khoshjahan, M. Moeini-Aghtaie and M. Fotuhi-Firuzabad, "Developing new participation model of thermal generating units in flexible ramping market," in *IET Generation, Transmission & Distribution*, vol. 13, no. 11, pp. 2290-2298, 4 6 2019.

[15] H. Wu, M. Shahidehpour, A. Alabdulwahab and A. Abusorrah, "Thermal Generation Flexibility With Ramping Costs and Hourly Demand Response in Stochastic Security-Constrained Scheduling of Variable Energy Sources," in *IEEE Transactions on Power Systems*, vol. 30, no. 6, pp. 2955-2964, Nov. 2015.

[16] R. Chen, J. Wang, A. Botterud and H. Sun, "Wind Power Providing Flexible Ramp Product," in *IEEE Transactions on Power Systems*, vol. 32, no. 3, pp. 2049-2061, May 2017.

[17] M. Cui, J. Zhang, H. Wu and B. Hodge, "Wind-Friendly Flexible Ramping Product Design in Multi-Timescale Power System Operations," in *IEEE Transactions on Sustainable Energy*, vol. 8, no. 3, pp. 1064-1075, July 2017.

[18] J. Hu, M. R. Sarker, J. Wang, F. Wen and W. Liu, "Provision of flexible ramping product by battery energy storage in day-ahead energy and reserve markets," in *IET Generation, Transmission & Distribution*, vol. 12, no. 10, pp. 2256-2264, 29 5 2018.

[19] G. Wang, Z. Xu, F. Wen, and K. P. Wong, “Traffic-constrained multiobjective planning of electric-vehicle charging stations,” *IEEE Trans. Power Del.*, vol. 28, no. 4, pp. 2363-2372, Oct. 2013.

[20] W. Yao, J. Zhao, F. Wen, Z. Dong, Y. Xue, Y. Xu, and K. Meng, “A multi-objective collaborative planning strategy for integrated power distribution and EV charging systems,” *IEEE Trans. Power Syst.*, vol. 29, no.4, pp. 1811-1821, Jul. 2014.

[21] S. Wang, Z. Y. Dong, F. Luo, K. Meng, and Y. Zhang, “Stochastic collaborative planning of EV charging stations and power distribution system”, *IEEE Trans. Ind. Informat.*, vol. 14, no. 1, pp.321-331, Jan. 2018.

[22] G. Wang *et al.*, "Robust Planning of Electric Vehicle Charging Facilities with an Advanced Evaluation Method," in *IEEE Transactions on Industrial Informatics*, vol. 14, no. 3, pp. 866-876, March 2018.

[23] G. Hinton, and R. Salakhutdinov, "Reducing the Dimensionality of Data with Neural Networks," *Science*, vol. 313, pp. 504-507, Jul. 2006.

[24] H. Wang, Z. Lei, X. Zhang, B. Zhou, J. Peng, "A review of deep learning for renewable energy forecasting, " in Energy Conversion and Management, vol.198, 2019, 111799.

[25] W. Huang, G. Song, H. Hong and K. Xie, "Deep Architecture for Traffic Flow Prediction: Deep Belief Networks With Multitask Learning," in *IEEE Transactions on Intelligent Transportation Systems*, vol. 15, no. 5, pp. 2191-2201, Oct. 2014.

[26] X. Luo, S. Xia, K. W. Chan and X. Lu, "A Hierarchical Scheme for Utilizing Plug-In Electric Vehicle Power to Hedge Against Wind-Induced Unit Ramp Cycling Operations," in *IEEE Transactions on Power Systems*, vol. 33, no. 1, pp. 55-69, Jan. 2018.

[27] B. Zhang and M. Kezunovic, "Impact on Power System Flexibility by Electric Vehicle Participation in Ramp Market," in *IEEE Transactions on Smart Grid*, vol. 7, no. 3, pp. 1285-1294, May 2016.

[28] K. Shaloudegi, N. Madinehi, S. H. Hosseinian, and H. A. Abyaneh, "A novel policy for locational marginal price calculation in distribution systems based on loss reduction allocation using game theory," in *IEEE Transactions on Power Systems*, vol. 27, no. 2, pp. 811–820, May 2012.

[29] J. Hu, S. You, M. Lind, and J. Østergaard, "Coordinated charging of electric vehicles for congestion prevention in the distribution grid," *IEEE Trans. Smart Grid*, vol. 5, no. 2, pp. 703–711, Mar. 2014.

[30] Geoffrey SO, Hinton E, Teh Y-W, "A fast learning algorithm for deep belief nets," *Neural Comput.*, vol. 18, no.7, pp. 1527–1554, Jul. 2006.

[31] H. Wang, G. Wang, G. Li, J. Peng, Y. Liu, "Deep belief network based deterministic and probabilistic wind speed forecasting approach," *Applied Energy*, vol. 182, pp. 80-93, Nov. 2016.

[32] G. Hinton, "Training products of experts by minimizing contrastive divergence," *Neural Comput.*, vol. 14, no. 8， pp. 1771-1800, Aug. 2002.

[33] G. E. Hinton, S. Osindero and Y. W. Teh, "A fast learning algorithm for deep belief nets," *Neural Computation*, vol. 18, no. 7, pp. 1527-1554, July 2006.

[34] Q. Wang and B. M. Hodge, "Enhancing Power System Operational Flexibility with Flexible Ramping Products: A Review," in *IEEE Transactions on Industrial Informatics*, vol. 13, no. 4, pp. 1652-1664, Aug. 2017.

[35] Energy Networks Australia, "Electricity network transformation roadmap: final report," [Online]. Available: https://www.energynetworks.com.au/resources/reports/entr-final-report/

[36] Australian Energy Market Commission, "How digitalization is changing the NEM: the potential to move to a two-sided market," [Online]. Available: https://www.aemc.gov.au/sites/default/files/2019-11/How%20digitalisation%20is%20changing%20the%20NEM.pdf

[37] H. Yuan, F. Li, Y. Wei and J. Zhu, "Novel Linearized Power Flow and Linearized OPF Models for Active Distribution Networks With Application in Distribution LMP," in *IEEE Transactions on Smart Grid*, vol. 9, no. 1, pp. 438-448, Jan. 2018.

[38] Y. Liu, J. Li and L. Wu, "Distribution System Restructuring: Distribution LMP via Unbalanced ACOPF," in *IEEE Transactions on Smart Grid*, vol. 9, no. 5, pp. 4038-4048, Sept. 2018.

[39] M. Hong, "An Approximate Method for Loss Sensitivity Calculation in Unbalanced Distribution Systems," in *IEEE Transactions on Power Systems*, vol. 29, no. 3, pp. 1435-1436, May 2014.

[40] E. A. Farsani, H. A. Abyaneh, M. Abedi and S. H. Hosseinian, "A Novel Policy for LMP Calculation in Distribution Networks Based on Loss and Emission Reduction Allocation Using Nucleolus Theory," in *IEEE Transactions on Power Systems*, vol. 31, no. 1, pp. 143-152, Jan. 2016.

[41] X. Yan, C. Gu, F. Li and Z. Wang, "LMP-Based Pricing for Energy Storage in Local Market to Facilitate PV Penetration," in *IEEE Transactions on Power Systems*, vol. 33, no. 3, pp. 3373-3382, May 2018.

[42] P. M. Sotkiewicz and J. M. Vignolo, "Nodal pricing for distribution networks: Efficient pricing for efficiency enhancing DG," *IEEE Trans. Power Syst.*, vol. 21, no. 2, pp. 1013–1014, May 2006.

[43] C. Gu, J. Wu, and F. Li, "Reliability-based distribution network pricing," *IEEE Trans. Power Syst.*, vol. 27, no. 3, pp. 1646–1655, Aug. 2012.

[44] H. K. Nguyen, A. Khodaei and Z. Han, "Incentive Mechanism Design for Integrated Microgrids in Peak Ramp Minimization Problem," in *IEEE Transactions on Smart Grid*, vol. 9, no. 6, pp. 5774-5785, Nov. 2018.

[45] A. Majzoobi and A. Khodaei, "Application of Microgrids in Supporting Distribution Grid Flexibility," in *IEEE Transactions on Power Systems*, vol. 32, no. 5, pp. 3660-3669, Sept. 2017.

[46] W. Yao, C. Y. Chung, F. Wen, M. Qin, and Y. Xue, "Scenario-based comprehensive expansion planning for distribution systems considering integration of plug-in EVs," *IEEE Trans. Power Syst.*, vol. 31, no.1, pp. 317-328, Jan. 2016.

[47] F. C. Schweppe, M. C. Caramanis, R. D. Tabors, R. E. Bohn, *Spot Pricing for Electricity*, MA, Boston: Kluwer, 1988.

[48] R. J. Green, "Competition in generation: The economic foundations", *Proc. IEEE*, vol. 88, no. 2, pp. 128-139, Feb. 2000.

[49] E. Ela and M. O'Malley, "Scheduling and Pricing for Expected Ramp Capability in Real-Time Power Markets," in *IEEE Transactions on Power Systems*, vol. 31, no. 3, pp. 1681-1691, May 2016.

[50] J. H. Zhao, Z. Y. Dong, P. Lindsay and K. P. Wong, "Flexible Transmission Expansion Planning with Uncertainties in an Electricity Market," in *IEEE Transactions on Power Systems*, vol. 24, no. 1, pp. 479-488, Feb. 2009.

[51] K. Qian, C. Zhou, M. Allan and Y. Yuan, "Modeling of Load Demand Due to EV Battery Charging in Distribution Systems," in *IEEE Transactions on Power Systems*, vol. 26, no. 2, pp. 802-810, May 2011.

[52] Highways England, *Traffic Flow Data*, [Online]. Available: http://tris.highwaysengland.co.uk/detail/trafficflowdata

[53] Highways England, *Monthly Summary Data*, [Online]. Available: http://tris.highwaysengland.co.uk/detail/monthlysummarydata

[54] S. Boyd and V. Lieven, *Convex optimization*. Cambridge University press, 2004.